Scripta Materialia 114 (2016) 98–102

Contents lists available at ScienceDirect

Scripta Materialia

journal homepage: www.elsevier.com/locate/scriptamat

Electrically conductive graphene nanoplatelet/boron carbide composites with high hardness and toughness

Yongqiang Tan, Haibin Zhang *, Shuming Peng *

Innovation Research Team for Advanced Ceramics, Institute of Nuclear Physics and Chemistry, China Academy of Engineering Physics, Mianyang 621900, China

ARTICLE INFO

Article history:
Received 25 October 2015
Received in revised form 17 November 2015
Accepted 5 December 2015
Available online 19 December 2015

Keywords:
Ceramic matrix composites
Spark plasma sintering
Electrical properties
Mechanical properties
Graphene nanoplatelet

ABSTRACT

B_4C composites containing 1–4 vol.% graphene nanoplatelet (GNP) were fabricated aiming at obtaining electrically conductive B_4C composites with high toughness. The electrical conductivity of B_4C composite was enhanced remarkably with the addition of only 2 vol.% GNPs. Besides, all the GNP/B_4C composites maintained high Vickers hardness. The fracture toughness kept increasing with the increase of GNPs volume fraction and a high value of 5.26 $MPa \cdot m^{1/2}$ was obtained in GNP/B_4C composite with 4 vol.% GNPs. The main toughening mechanisms include GNPs pull-out, crack deflection and crack bridging.

Boron carbide (B_4C) ceramics exhibit excellent properties such as low density, exceptionally high hardness and good wear resistance. Therefore, they become attractive materials for multiple applications in abrasive media, cutting tools and light weight armors [1–3]. More importantly, B_4C ceramics are extensively used in the nuclear reactors as control rods, shielding materials and as neutron detectors because of the presence of isotope ^{10}B which owns a high neutron absorption cross-section over a wide range of neutron energies [1–3]. They are the leading control rod materials in liquid-metal-cooled fast breeder reactors (LMFBR) and boiling water reactors (BWR).

Currently, the fabrication of dense B_4C ceramics relies on pressure-assisted sintering methods as hot-press sintering and spark plasma sintering (SPS) due to their poor sinterability [1]. However, it is quite difficult to fabricate B_4C ceramics with complex geometries using those pressure-assisted sintering methods. Further, to machine B_4C ceramics into intricate parts using traditional cutting techniques is also challenging and costly owning to their extremely high hardness and brittleness. In order to improve the machinability of B_4C ceramics, hexagonal boron nitride (h-BN) has been incorporated into B_4C [4]. Although the B_4C/h-BN composites with more than 20 wt.% h-BN exhibited significantly enhanced machinability, their Vickers hardness decreased to a much lower level [4]. Electrical discharge machining (EDM) is an attractive alternative machining technique which enables the low cost and highly flexible manufacture of hard ceramics without deteriorating their unique hardness [5]. However, the relatively low electrical conductivity of monolithic B_4C ceramics does not suffice to enable the EDM. Consequently, electrically conductive B_4C ceramics are especially interesting and greatly desirable for the use of EDM.

One of the most common means to enhance the electrical conductivity of insulating materials is to incorporate conducting particles into these insulating matrices. However, due to the low aspect ratio, the volume content of conventional conducting particles for an electrically percolating network was usually quite high. For example, over 25 vol.% conductive titanium diboride (TiB_2) was needed to percolate B_4C ceramic matrix and to achieve a considerable electrical conductivity enhancement [6]. However, such a high TiB_2 content was detrimental to both the low density and mechanical properties of B_4C ceramics. In recent years, graphene nanoplatelet (GNP), a new two-dimensional (2-D) carbon nanostructure material which consists of a few graphene layers, has become one of the most effective nanofillers for electrically conductive ceramic composites due to its outstanding electrical properties and high aspect ratio [7–9]. A reasonably low GNPs volume content was sufficient for the electrical percolation of an insulating ceramic matrix and thus the other properties of the ceramic matrix, especially the hardness, can be well maintained or even improved [7–9]. It was reported that the incorporation of 3 vol.% GNPs into insulating Al_2O_3 matrices could give rise to increments of up to 14 orders of magnitude in electrical conductivity [7,10]. Compared with its counterpart carbon nanotube (CNT), GNP shows much better dispersability and lower cost. Besides, GNP/ceramic composites exhibited significantly improved toughness compared with monolithic ceramics [11–15]. The toughening mechanisms include sheet pull-out, two- and three-dimensional crack deflection and crack bridging et al. [11–15]. Therefore, it is promising to obtain enhanced electrical conductivity and mechanical properties simultaneously by fabricating GNP/B_4C composite. Nevertheless, to the best of

---

* Corresponding authors.
E-mail addresses: hbzhang@caep.cn (H. Zhang), pengshuming@caep.cn (S. Peng).

http://dx.doi.org/10.1016/j.scriptamat.2015.12.008

our knowledge, no study on electrical properties of B_4C composites containing GNPs has been reported so far.

In this study, GNP/B_4C composites containing different GNP contents were fabricated by colloidal processing and SPS. SPS is an effective sintering method for dense ceramics at relatively low temperatures; therefore, it can promote densification of B_4C composites effectively and avoid the thermally induced structural damage to the GNPs. The microstructure and distribution of GNPs in the composites as well as the influence of GNPs on the electrical and mechanical properties of GNP/B_4C composites were systematically studied.

GNPs used in this study were purchased from Deyang Carbonene Technology Co., Ltd. The platelets are stacks of graphene sheets about 6–8 nm in thickness and 1–5 μm in level dimensions. Different amounts of GNPs were first dispersed in isopropanol with a concentration of 0.1 mg/mL and sonicated for 2 h. B_4C powders (Grade HS, H. C. Starck GmbH, Germany) were then added to the GNPs dispersions gradually and stirred in an ultrasonic bath for 12 h. The solvent was removed at 85 °C in a rotary-evaporator and the slurry was then dried and sieved. The powders were placed in a 15 mm diameter graphite die and sintered using the spark plasma sintering furnace (Labox-325, Japan). All the samples were sintered at 1800 °C for 3 min with a uniaxial pressure of 80 MPa. Density of the sintered samples was determined by the Archimedes method. The electrical conductivity was measured by the four-terminal method. The microstructural characterizations of the samples were determined by scanning electron microscopy (SEM) and Raman spectroscopy. The Vickers hardness was determined by the Vickers diamond indentation method using the following equation:

$$H_v = 1.854 \times 10^{-9} \frac{P}{d^2} \tag{1}$$

where P is the indentation load (9.8 N in this study) load on the polished surface and d is the average diagonal length of the Vickers indentation. Indentation fracture toughness values of the specimens were semiquantitatively estimated from observed corner cracks and calculated Vickers hardness using the Anstis equation [16]:

$$K_{IC} = 0.016 \left(\frac{E}{H}\right)^{1/2} \left(\frac{P}{c_0^{3/2}}\right) \tag{2}$$

where E is the Young's modulus which was determined by the resonance method and c_0 is the half-length of cracks formed by the indentation.

Table 1 summarizes the density of the GNP/B_4C composites with different GNP contents. The theoretical density was calculated by the rule of mixtures assuming densities of 2.52 g/cm^3 and 2.20 g/cm^3 for B_4C and GNPs respectively. It can be seen that all composites could be densified to around 99% of their theory densities after SPS at 1800 °C, demonstrating that SPS is a very effective technique to promote the densification of B_4C ceramics. The sintering temperature for fully dense GNP/B_4C composites is in good consistence with the sintering temperature for SPSed B_4C ceramics reported in literature [17,18] and much lower than that of hot-press sintering [19]. Due to the relatively low GNPs concentration, the sinterability of B_4C was almost not influenced by the addition of GNPs.

Table 1
Densities of GNP/B_4C composites SPSed at 1800 °C.

GNPs content (vol.%)	Sintering temperature (°C)	Density (g/cm^3)	Theoretical density (g/cm^3)	Relative density (%)
0	1800	2.502	2.520	99.2
1	1800	2.500	2.517	99.2
2	1800	2.501	2.514	99.4
4	1800	2.494	2.507	98.5

Raman spectra were collected on the polished surfaces both parallel and perpendicular to the SPS pressing axis of the GNP/B_4C composites with 2 and 4 vol.% GNPs and the results are shown in Fig. 1, together with the Raman spectroscopy of the as-received GNPs. The peaks at 1340 cm^{-1} (D band) and 1589 cm^{-1} (G band) are the main features of sp^2 crystalline graphitic structures [20]. The peak at 2660 cm^{-1} (G' band) reveals the few-layer nature of GNPs in as-received state and in B_4C composites [21,22]. The relative lower G' band in the composites suggest the possible overlapping of GNPs. Compared with as-received GNPs, the intensity of the D band, characteristic of disorder, became much higher in GNP/B_4C composites, especially for surfaces parallel to the SPS pressing axis. Meanwhile, D' and D + D' bands which were also indicators of defective graphene [22] appeared in the GNP/B_4C composites besides the peaks corresponding to B_4C. The defective nature of GNPs in the composites may be ascribed to the contribution of the exposed platelets edges. Since GNPs tended to align perpendicular to the SPS pressing axis during sintering, which will be shown in the following part, more edges were expected on the surface parallel to the SPS pressing axis of the composites. This assumption can be demonstrated by the clearly lower D band of the Raman spectra on surface perpendicular to the SPS pressing axis. Besides, the reaction between GNPs and the oxide layer of B_4C at high temperatures could also induce certain defects.

Fig. 2 shows the fracture surface of GNP/B_4C composites with different GNP concentrations. It can be seen that all these composites showed fully dense microstructures. The fracture mode of B_4C grains was dominantly transgranular, which explains the low fracture toughness of monolithic B_4C ceramics. GNPs can be clearly distinguished in GNP/B_4C composites, as indicated in Fig. 3(b)–(c). For GNP/B_4C composites containing relatively lower concentration of GNPs, the GNPs were uniformly distributed in B_4C matrices (Fig. 2(b) and (c)). For GNP/B_4C composite containing 4 vol.% GNPs, a slight degree of aggregation was occasionally observed, as indicated in Fig. 2(d). The higher resolution SEM image in Fig. 2(e) illustrates the GNPs that typically run along and wrapped around the grain boundaries of the matrix respectively in the composite with 4 vol.% GNPs. Generally, the GNPs were protruding out of the fracture surface. The GNPs pull-out was also observed as shown in Fig. 2(f). The GNPs in B_4C matrices tended to align parallel to each other due to the high pressure during sintering, which is consistent with previous reports [8,9,14]. The level dimensions of GNPs in composite with 1 vol.% GNPs were consistent with those of the as-received GNPs. While the GNPs in composites with higher GNPs content showed a larger level dimension due to the possible overlapping between adjacent sheets which was essential for a percolating network. This kind of overlapping was also suggested by Raman spectra in Fig. 1.

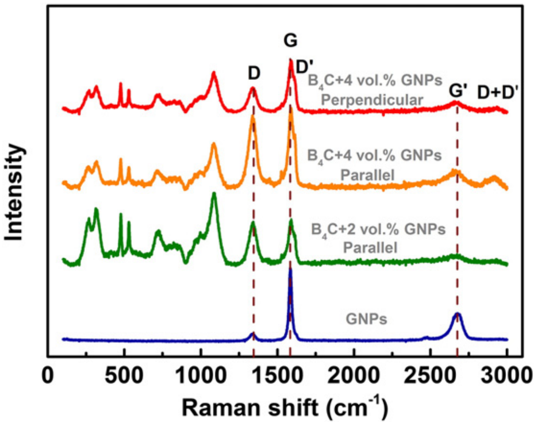

Fig. 1. Raman spectra of as-received GNPs and GNP/B_4C composites.